Design flood estimation for global river networks based on machine learning models

Gang Zhao[1], Paul Bates[1,2], Jeffrey Neal[1,2], Bo Pang[3]

[1] School of Geographical Sciences, University of Bristol, Bristol, UK
5 [2] Fathom, Engine Shed, Station Approach, Bristol, UK
[3] College of Water Sciences, Beijing Normal University, Beijing, China

Correspondence to: Gang Zhao (gang.zhao@bristol.ac.uk)

Abstract. Design flood estimation is a fundamental task in hydrology. In this research, we propose a machine learning based
10 approach to estimate design floods globally. This approach mainly involves three stages: (*i*) estimating at-site flood frequency
curve for global gauging stations by the Anderson-Darling test and Bayesian MCMC method; (*ii*) clustering these stations into
subgroups by a K-means model based on twelve globally available catchment descriptors, and (*iii*) developing a regression
model in each subgroup for regional design flood estimation using the same descriptors. A total of 11793 stations globally
were selected for model development and three widely used regression models were compared for design flood estimation.
15 The results showed that: (1) the proposed approach achieved the highest accuracy for design flood estimation when using all
twelve descriptors for clustering; and the performance of regression was improved by considering more descriptors during the
training and validation; (2) a support vector machine regression provide the highest prediction performance among all
regression models tested, with root mean square normalised error of 0.708 for 100-year return period flood estimation; (3)
100-year design flood in tropical, arid, temperate, cold and polar climate zones could be reliably estimated with the relative
20 mean relative biases (RBIAS) of -0.199, -0.233, -0.169, 0.179 and -0.091 respectively; (4) This machine learning based
approach shows considerable improvement over the index-flood based method introduced by Smith et al. (2015,
https://doi.org/10.1002/2014WR015814) for the design flood estimation at global scales; and the average RBIAS in estimation
is less than 18% for 10, 20, 50 and 100-year design floods. We conclude that the proposed approach is a valid method to
estimate design floods anywhere on the global river network, improving our prediction of the flood hazard, especially in
25 ungauged areas.

1 Introduction

Flood hazard is the primary weather-related disaster worldwide, affecting 2.3 billion people and causing 662 billion US dollars
in economic damage between 1995 and 2015 (CRED and UNISDR, 2015). The frequency and severity of flood events are
expected to increase in the future because of climate change and socio-economic growth in flood-prone areas (Kundzewicz et
30 al., 2014;Wing et al., 2018a;Winsemius et al., 2016a;Wing et al., 2017;Winsemius et al., 2016b;Wing et al., 2018b). Flood

hazard models are mature tools to identify flood-prone areas and have been widely used in flood risk management at catchment or regional scales (Hammond et al., 2015;Teng et al., 2017). With the development of new remote sensing techniques and an increase in computing power, global flood hazard models (GFHMs) are now a practical reality and have been successfully applied for large-scale flood mapping and validated in several countries (Sampson et al., 2015;Schumann et al., 2013). GFHMs

35 can identify flood-prone areas in ungauged basins and provide a consistent and comprehensive understanding of the flood hazard at national, continental and global scales.

The 'cascade' model type and 'gauged flow data' model type are the two most frequently used approaches in global flood hazard modelling and both map the flood hazard based on return period flows (Trigg et al., 2016). The cascade model type, for example CaMa-UT (Yamazaki et al., 2011) and GLOFRIS (Winsemius et al., 2013), uses land surface models driven by

40 climate reanalysis data to simulate streamflow. Return period flows along the river network in the cascade model type are derived by an at-site flood frequency analysis of the resulting land surface model streamflow. However, due to the coarse resolution (usually 0.5 degrees) of global land surface models (Yang et al., 2019b;Liu et al., 2019), some downscaling and bias correction methods usually need to be adopted for high-resolution flood hazard mapping (Mueller Schmied et al., 2016;Frieler et al., 2017;Schumann et al., 2014a). Unlike the cascade model type, the gauged flow data model type uses observed gauged

45 discharge and regional flood frequency analysis (RFFA) approaches to produce different return period flows along the global river network (Trigg et al., 2016). Compared with the cascade model type, the gauged flow data model type can be preferable for high-resolution flood hazard mapping as it avoids the uncertainties from land surface model implementation (Prihodko et al., 2008) and flood map downscaling (Schumann et al., 2014b). However, the performance of the RFFA approach adopted is highly dependent on the coverage and density of observed discharge stations (Hosking and Wallis, 1988;Lin and Chen, 2006).

50 RFFA has long been regarded as a reliable method to estimate design floods in engineering hydrology (Cunnane, 1988). Based on the basic assumption that there is a relationship between catchment descriptors and the design flood in a region, different types of RFFA approaches have been proposed and successfully applied in regional studies in the past five decades (Griffis and Stedinger, 2007;Merz and Bloschl, 2008a, b;Dalrymple, 1960). Amongst these, the index-flood method and the direct regression method are two of the most widely used procedures (Shu and Ouarda, 2008). The index-flood method assumes that

55 the flood frequency curves at different sites in a region are identical except for one scale index (named as the index-flood) (Dalrymple, 1960;Bocchiola et al., 2003). Therefore, the index-flood method involves two steps; index-flood estimation and derivation of a single regional flood frequency relationship, often termed a growth curve. Unlike the index-flood method, the direct regression method predicts flood quantiles as a function of catchment descriptors directly (Shu and Ouarda, 2008). These two methods have been successfully applied at both regional and national scales (Salinas et al., 2013), but very few applications

60 of such methods have been performed at the global scale. To the best of our knowledge, only Smith et al. (2015) have proposed an RFFA approach at the global scale based on the index-flood method (termed global RFFA). This approach has been applied successfully in high-resolution flood hazard mapping for ungauged areas in several countries (Sampson et al., 2015;Wing et al., 2017).

However, the global RFFA approach of Smith et al (2015) has shown some deficiencies during application and which we seek to address in this research as follows:

(1) the global RFFA approach of Smith et al (2015) was developed based on 945 stations in the Global Runoff Data Base (GRDB) and the United States Geological Survey (USGS) database. This limited number of stations means that it cannot provide a reliable estimation in some regions at global scale. To improve the coverage and density of discharge stations, nearly 12,000 stations from the newly published Global Streamflow Indices and Metadata (GSIM) archive were selected for model development in this research.

(2) the flood frequency curve in the Smith et al (2015) approach was assumed to obey a GEV distribution for the global coverage. Studies have suggested alternate distributions, such as generalized pareto distribution, perform better in populated regions of Australia and a log pearson type 3 distribution was recommended in the southwestern United States (Vogel et al., 1993a;Vogel et al., 1993b). In this research, the at-site flood frequency curve was selected from eight widely used distributions based on the Anderson-Darling goodness of fit tests;

(3) the global RFFA approach of Smith et al. (2015) adopted only three catchment descriptors (rainfall, slope and catchment area) for clustering and flood estimation. These three factors can only provide a basic description of global catchment characteristics. In this research, twelve catchment descriptors covering meteorological, physiographical, hydrological and anthropological aspects were considered for clustering and design flood estimation.

(4) the global RFFA approach of Smith et al. (2015) was proposed based on the index-flood method and the index-flood in ungauged areas was computed with a power-form function. As the coefficient of variation of flood flows generally varies from site to site, the index-flood method is not recommended if available samples contain more than 10 observations or are highly cross-correlated (Stedinger, 1983). Moreover, the simple power-form function may fail to capture complicated relationships within the data, since the relationship between flood and each descriptor is assumed to obey an explicit power-form function which may not be always be appropriate. In this research, the regional flood is estimated based on direct regression method and machine learning models were adopted to describe the unknown relationship between catchment descriptors and at-site design floods. These machine learning based method have shown advantages over ordinary regression approaches in RFFA at regional scales (Gizaw and Gan, 2016;Shu and Ouarda, 2008;Zhang et al., 2018), and are tested here for the first time in a global study.

The aim of this research is therefore to provide an improved method for reliable design flood estimation addressing the deficiencies identified with the previous global scale study of Smith et al (2015). A three-phase model framework is applied where Bayesian MCMC, K-means and SVM models were applied for at-site flood estimation, subgroup delineation and regional flood estimation, respectively. Specifically, 11,793 stations selected from the GSIM archive are used for model development and the stations were divided into 16 subgroups using a K-means model and twelve catchment descriptors. For each subgroup, 70% and 30% stations were randomly selected for model training and validation respectively. Three types of regressions including Power Form function (PF), Support Vector Machine (SVM) and Random Forest (RF) were compared

for regional flood estimation. Finally, the proposed direct regression approach is compared with the previous results of Smith et al. (2015) in each climate zone.

2 Study areas and data

100 ### 2.1 Flood data

Observed annual maximum streamflow data in the GSIM archive were used to estimate at-site design floods (DFs) at different return periods. This archive is a collection of streamflow indices that includes more than 35,000 stations from seven national and five international streamflow databases (Gudmundsson et al., 2018;Do et al., 2018). Compared with a widely used database in large-scale hydrological studies, such as the Global River Discharge Database (GRDB) which contains data from 9500

105 stations, the GSIM archive can help to improve the understanding of large-scale hydrological processes by improving the coverage and density of streamflow observations. After quality control of the daily streamflow data, 15 types of time-series indices are provided at yearly, seasonal, and monthly resolutions in the GSIM archive. To date, this archive has been successfully used in flood classification (Stein et al., 2019), streamflow trend analysis (Do et al., 2019) and hydrological model evaluation (Yang et al., 2019a) at the global scale.
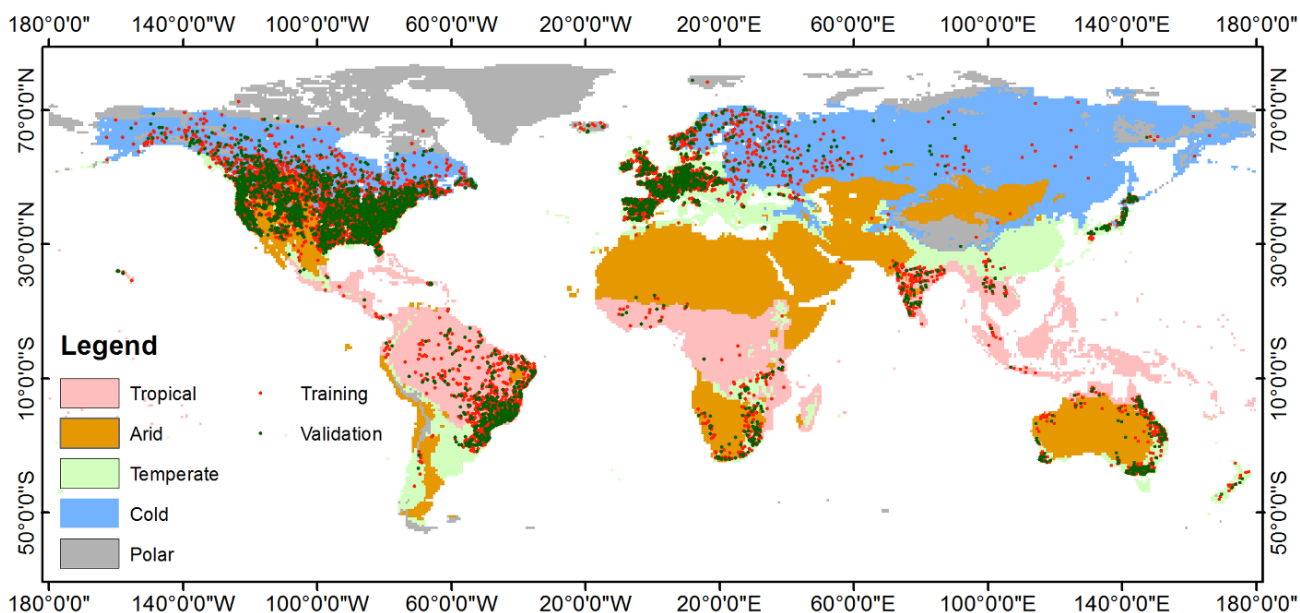
110

Figure 1 The distribution of discharge stations used for training and validation in this research.

To make reliable estimates for at-site DFs, a station selection is needed based on some quality control criteria. Firstly, the ranges of streamflow parameters are reported to narrow substantially with at least 20 years of record (Richter et al., 1997). Therefore, only stations with a historical streamflow record of 20 years or longer were selected for the analysis. Second, the

115 RFFA approach requires the assumption of flood stationarity. Stations experiencing obvious trends or sudden changes were detected by a Mann-Kendall test (MKT) (Hamed, 2008) and the standard normal homogeneity test (SNHT) (Alexandersson, 1986). Any stations exhibiting obvious non-stationarity, or which do not obey the given hypothetical distributions were not considered further in model development. Lastly, to better estimate DFs at the global scale, the selected stations were first divided into several sub-groups based on a K-means clustering model, and separate regression models were developed for the

120 different sub-groups. The streamflow stations in each sub-group were also required to pass discordancy and heterogeneity tests. The adopted stationarity, discordancy and heterogeneity measures are described in Section 3 and the distribution of training and validation stations after selection is shown in **Figure 1.**

Table 1 compares the number of stations used for model training and validation in each climate class between Smith et al. (2015) and this study. Compared with the research of Smith et al. (2015), the number of stations in this research is significantly

125 improved in all climate classes.

Table 1 The number of discharge stations for model development in each climate class

Climate Class	Smith et al. (2015)		This research	
	Training	Validation	Training	Validation
Tropical	163	8	716	298
Arid	121	55	595	231
Temperate	296	99	4231	1816
Cold	109	80	2666	1099
Polar	14	N/A	100	41
Total	703	242	8308	3485

2.2 Catchment descriptors

The main idea of an RFFA is to characterise a relationship between at-site DFs and catchment descriptors and then apply this relationship to estimate flood magnitudes along the river network in similar ungauged catchments. In this research, the river

130 network of the global coverage is extracted from the 1km resolution catchment area map for catchments exceeding a threshold area of 50 km^2. Twelve explanatory factors collected from open-access databases were selected as potential descriptors and applied for clustering and regression model development. The statistics and data sources of these factors are summarised in **Table 2**.

Table 2 Statistics and data source of the explanatory descriptors

No.	Factor name (Abbreviation)	Unit	Min	Max	Data source
1	Annual Precipitation (AP)	mm	0	7743	WorldClim
2	Precipitation Seasonality (PS)	-	0	219.35	WorldClim

3	Annual Mean Temperature (AT)	°C	-27.57	33.44	WorldClim
4	Temperature Annual Range (TR)	°C	0	74.79	WorldClim
5	Mean Slope (SL)	degree	0	32.78	MERIT DEM
6	Lake fraction (LF)	%	0	1	GLWD
7	Longitude (LO)	degree	-180	180	WGS 84
8	Latitude (LA)	degree	-60	85	WGS 84
9	Curve number (CN)	-	0	95	NRCS CN dataset
10	Catchment area (CA)	km^2	50	16198686	MERIT DEM
11	Dam capacity (DC)	million m^3	0	2648	GRanD
12	Population density (PD)	number/km^2	0	5317	GPW

135 These explanatory factors can be grouped into four categories as follows:

(1). *Meteorological factors* included annual precipitation (AP), precipitation seasonality (PS), annual mean temperature (AT), and annual temperature range (TR). AP and AT represent the average annual precipitation and mean temperature of the upstream catchment respectively. PS is the coefficient of variation of the monthly rainfall series and TR is the range between the maximal and minimal temperatures of the time series average over the upstream catchment. These four factors were
140 collected from the WorldClim dataset (V2) at 30 arcsecond (~1km) resolution (Fick and Hijmans, 2017) and are used to represent the extreme value and seasonal distribution of precipitation and temperature.

(2). *Physiographical factors* comprised discharge station location, slope (SL) and lake fraction (LF) of the upstream catchment. Station location is defined by the longitude (LO) and latitude (LA) of the discharge station in degree units of the World Geodetic System 1984 (WGS84) spatial reference frame. SL reflects the average slope of the upstream catchment which is
145 calculated based on the MERIT DEM (Yamazaki et al., 2017). LF represents the fraction of the catchment area upstream of the station covered with lakes. The location and area of global lakes are taken from the Global Lakes and Wetlands Database (GLWD) (Lehner and Doll, 2004).

(3). *Hydrological factors* Catchment area (CA) and Curve Number (CN) reflect the area and runoff capacity of the upstream catchment respectively. CA is defined as the upstream flow accumulation area based on the D8 algorithm and the Merit DEM.
150 CN is an empirical parameter for runoff prediction in ungauged areas which is calculated from the tables in the National Engineering Handbook of the United States, Section-4 (NEH-4) (Mockus, 1964). The CN in this research is collected from a global CN dataset that utilizes the latest Moderate Resolution Imaging Spectroradiometer (MODIS) land cover information and the Harmonized World Soil Database (HWSD) soil data (Zeng et al., 2017).

(4). *Anthropological factors* include total dam capacity (DC) and population density (PD). DC is the total dam capacity of the
155 upstream catchment. The location and capacity of each dam is provided by the Global Reservoir and Dam (GRanD) dataset
which includes about 7000 dams globally (Lehner et al., 2011). PD is a widely used factor to reflect the impact of human
activities on the environment. The PD map in this research is collected from the Gridded Population of the World (GPW)
dataset as of the year 2015 (Doxsey-Whitfield et al., 2015).

3 Methodology

160 The flowchart for this research has three parts which are shown in **Figure 2**. Part (a) includes the procedures of station selection
and at-site design flood estimation that are described in Sections 3.1 and 3.2 respectively. Part (b) displays the procedure for
subgroup delineation by using a K-means clustering model (in Section 3.3). Part (c) describes the procedure of regression
model development and regional flood estimation in ungauged areas. Three regression models described in Section 3.4, were
adopted for model comparison.
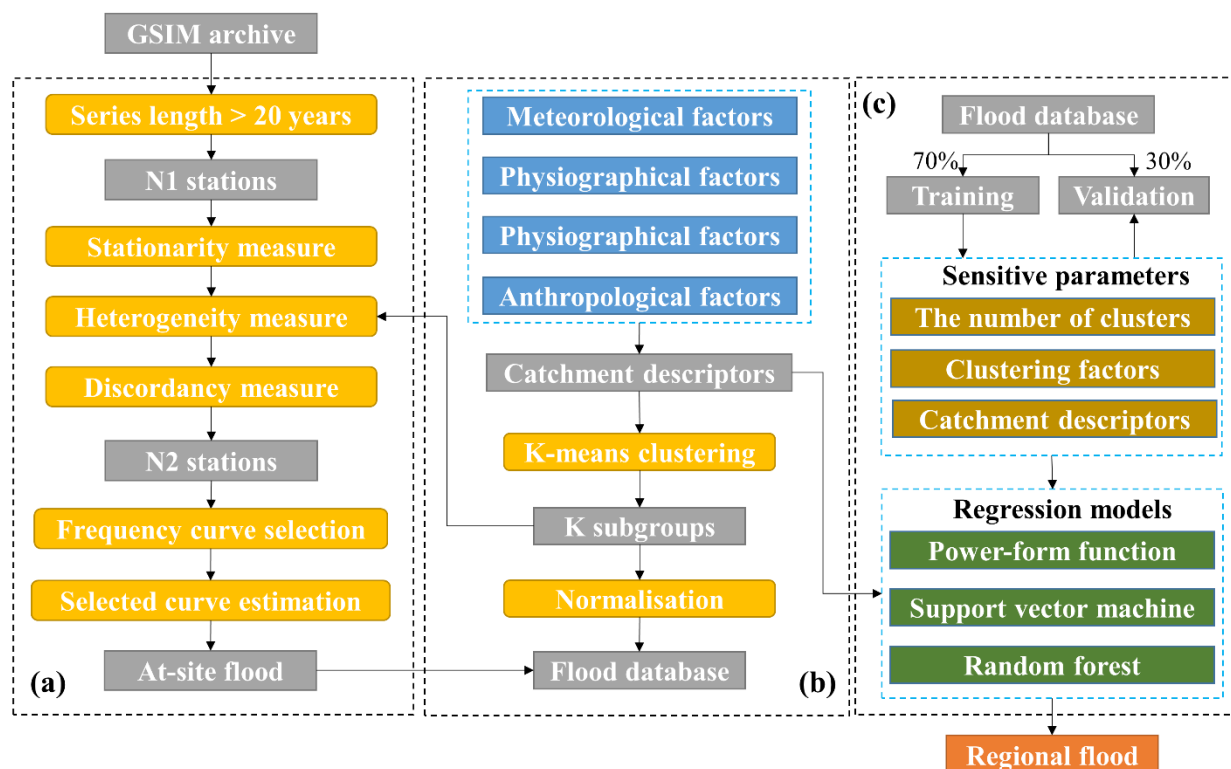
165

Figure 2 The framework of this research
(a) at-site flood estimation; (b) subgroups delineation; (c) regional flood estimation

3.1 Station selection methods

3.1.1 Stationarity measures

170   Two widely used stationarity measures in hydrology, the Mann-Kendall test (MKT) (Hamed, 2008) and the standard normal homogeneity test (SNHT) (Alexandersson, 1986), were adopted for trend and change-point detection respectively in the research. For a discharge series $\{Y_i | i = 1,2,...,n\}$, the process of MKT is described in Eq. (1) to (4):

$$S = \sum_{i=1}^{n-1} \sum_{j=i+1}^{n} sgn(Y_j - Y_i), \tag{1}$$

$$sgn(y) = \begin{cases} 1, & y > 0 \\ 0, & y = 0, \\ -1, & y < 0 \end{cases} \tag{2}$$

175   The variance of S is computed as follows:

$$Var(s) = \frac{1}{18}(n(n-1)(2n+5) - \sum_{i=1}^{n} t_i i(i-1)(2i+5)), \tag{3}$$

Where n is the total number of time series Y_i; $Var(s)$ is the variance of S; t_i is the number of data points contained in the i-th tie group;

The MKT statistic Z is given by:

180    $$Z = \begin{cases} \frac{S-1}{\sqrt{Var(s)}}, & S > 0 \\ 0, & S = 0, \\ \frac{S+1}{\sqrt{Var(s)}}, & S < 0 \end{cases} \tag{4}$$

The SNHT is described in Eq. (5) to (8).

$$T_d = d\bar{z}_1^2 + (n-d)\bar{z}_2^2, d = 1,2,...n,, \tag{5}$$

$$\bar{Z}_1 = \frac{1}{d}\sum_{i=1}^{d}(Y_i - \bar{Y})/s, \tag{6}$$

$$\bar{Z}_2 = \frac{1}{n-d}\sum_{i=d+1}^{n}(Y_i - \bar{Y})/s, \tag{7}$$

185   The SNHT statistic T is given by:

$$T = max(T_d), \tag{8}$$

One advantage of these two tests is that they provide an index reflecting the degree of trend or change. The Z index in the MKT test was used to evaluate the trend of descending (negative values) and ascending (positive values) in the time series. The change-points occurred at the largest value of T among the time series T_d, and a larger T represents a higher change. After

190   stationarity measures were evaluated, each station has corresponding Z_i and T_i indices. The stations experiencing obvious trends and/or sudden changes were removed based on the 95% quantile value of the $|Z_i|$ and T_i indices.

3.1.2 Discordancy measures

The aim of using the discordancy measures was to detect potential outliers in each subgroup. Two discordancy measures are applied in this research to the time series of observed discharge. The first is the Z-score method (Shiffler, 1988) which is based on the value of mean annual runoff (R). The global gauging stations are divided into several subgroups and the R in each subgroup is normalised using Eq. (9) and z_i values greater than 3 are regarded as outliers (Garcia, 2012).

$$z_i = \frac{R_i - \overline{R}}{sd(R)}, \tag{9}$$

Where R_i is the mean annual runoff of station i in one subgroup, $\overline{R}$ is the mean value of R_i and $sd(R)$ is the standard deviation of R_i.

Another discordancy measure was proposed by Hosking and Wallis based on L-moments ratios (Hosking and Wallis, 2005). The discordancy of each station can be evaluated by D_i as defined in Eq. (10) to (12). As suggested by Hosking and Wallis, a station is considered as discordant if $D_i \geq 3$ when N_k is larger than 15.

$$D_i = \frac{1}{3} N_k (U_i - \overline{U})^T S^{-1} (U_i - \overline{U}), \tag{10}$$

$$\overline{U} = \frac{1}{N_k} \sum_1^{N_k} U_i, \tag{11}$$

$$S = \sum_1^{N_k} (U_i - \overline{U})(U_i - \overline{U})^T, \tag{12}$$

Where N_k is the number of stations in cluster k, and $U_i = [t^i, t_3^i, t_4^i]$ is the vector of L-CV, L-skewness and L-kurtosis of the station i as defined by Hosking and Wallis (2005).

3.2 At-site flood estimation

The at-site flood estimation involves two steps. Firstly, the flood frequency curve for each station was selected from eight widely used hypothetical distributions based on the Anderson-Darling goodness of fit test. **Table 3** describes the adopted hypothetical distributions. After the preferred distribution was selected, the parameters and design floods for this station were derived by a Bayesian MCMC method. The adopted Anderson-Darling test and Bayesian MCMC method are briefly described as follows.

Table 3 Hypothetical distributions adopted in this research

No.	Hypothetical distributions	Probability density function f(x) or cumulative distribution function F(X)
1	Normal distribution (NORM)	$f(x) = \frac{1}{\sqrt{2\pi b^2}} \exp\left(-\frac{(x-a)^2}{2b^2}\right)$

2	Exponential distribution (EXP)	$F(x) = 1 - \exp(-\dfrac{x-a}{b})$
3	Gumbel distribution (GUMBEL)	$F(x) = \exp[-\exp(-\dfrac{x-a}{b})]$
4	Generalized extreme value distribution (GEV)	$F(x) = \exp[-(1-\dfrac{b}{a}(x-c))^{\frac{1}{b}}]$
5	Generalized logistic distribution (GENLOGIS)	$F(x) = \dfrac{1}{(1+\exp(\frac{x-a}{b}))^c}$
6	Generalized Pareto distribution (GENPAR)	$F(x) = 1 - (1+c(\dfrac{(x-a)}{b}))^{-\frac{1}{c}}$
7	Lognormal distribution (LN3)	$f(x) = \dfrac{1}{\sqrt{2\pi}b(x-c)}\exp(-\dfrac{1}{2}(\dfrac{\log(x-c)-b}{a})^2)$
8	Pearson type III distribution (P3)	$f(x) = \dfrac{1}{a\Gamma(b)}\left(\dfrac{x-c}{a}\right)^{b-1}\exp\left(-\left(\dfrac{x-c}{a}\right)\right)$

Note: x is the random variable; a, b, c are parameters of distributions

3.2.1 Distribution selection

The Anderson-Darling (AD) test can detect whether a given sample of data follows a hypothetical distribution. Given a sample of data x_i ($i = 1,2, \ldots, m$), the AD test compares the cumulative frequency function of $F_m(x)$ and hypothetical distribution $F(x, \theta)$ as Eq. (13) to (15), where θ is the parameter estimated by the sample x_i.

$$\begin{cases} F_m(x) = 0, x < x_{(1)} \\ F_m(x) = \dfrac{i}{m}, x_{(i)} \leq x < x_{(i+1)}, \\ F_m(x) = 1, x_{(m)} \leq x \end{cases} \tag{13}$$

$$Q^2 = m \int_x [F_m(x) - F(x,\theta)]^2 \Psi(x)\, dF(x), \tag{14}$$

$$\psi(x) = \left[F(x,\theta)\left(1 - F(x,\theta)\right)\right]^{-1}, \tag{15}$$

Where: $x_{(i)}$ is the i-th element of sample in increasing order; the AD test statistic A^2 can be calculated as in Eq. (16) (Ahmad et al., 1988; Laio, 2004).

$$A^2 = -m - \frac{1}{m}\sum_{i=1}^{m}\{(2i-1)\ln[F(x_{(i)},\theta)] + (2m+1-2i)\ln[1-F(x_{(i)},\theta)]\}, \tag{16}$$

The AD statistic is widely used in flood frequency analysis as it shows good skill for small sample sizes and heavy-tailed distributions (Haddad and Rahman, 2011). For each station i, the A^2 statistic was calculated for all hypothetical distributions and the distribution with the minimum A^2 was selected as the flood frequency curve for that station. After selection of flood

frequency curve for all stations, a threshold $A^2_{95\%}$ was determined by the 95% quantile value of A^2_i. The stations at which A^2_i exceeded the threshold were regarded as not obeying all hypothetical distributions and these stations were not considered

230   further for model development.

3.2.2 Parameter estimation

The three common methods for estimating the parameters of at-site flood frequency curve are based on moments (MOM), maximum likelihood (MLE) and Bayesian inference. The adopted Bayesian MCMC method was proposed by Reis and Stedinger (2005) and is reported to provide better parameter estimates than the MOM and MLE approaches in some studies

235   (Nazmi et al., 2020;Haddad and Rahman, 2011;Gaume, 2018). The Bayesian MCMC approach derives an empirical approximation of the posterior distribution of parameters and flood quantiles for the selected distribution. The posterior distribution is computed using Bayesian inference as in Eq. (17).

$$P(\theta|D) = \frac{l(D|\theta)\xi(\theta)}{\int l(D|\theta)\xi(\theta)\,d\theta},$$ (17)

Where D is the given sample; θ is a parameter vector; $P(\theta|D)$ is the posterior distribution of the parameters θ; $\xi(\theta)$ is the

240   prior distribution of parameters θ; $l(D|\theta)$ is the likelihood function.

As the integral in Eq. (17) is insolvable analytically in practise, the Metropolis-Hastings MCMC method was used to generate samples from the posterior distribution. The detail of the Bayesian MCMC method is comprehensively described in the research of Reis and Stedinger (2005).

3.3 Clustering method

245   ### 3.3.1 K-means model

The standard K-means model was adopted for clustering in this research. This model has been widely used in the area of hydrology including in RFFA studies (Smith et al., 2015;Lin and Chen, 2006). The K-means model consists of two steps:

(a)   An input dataset $D = \{x_j | j = 1,2,3 \dots, N\}$ where N is the number of samples. The K centroids $C = \{C_k | k = 1,2,3 \dots, K\}$ are first randomly selected from the input dataset D. Each sample x_j is assigned to its nearest C_k based on the squared

250   Euclidean distance as in Eq. (18).

$$\arg\min_{c_k \in C} [dis(C_k, x_j)]^2,$$ (18)

Where: $dis(-)$ is the function for Euclidean distance calculation.

(b)   The centroid C_k in step (a) is updated as in Eq. (19). Then, the algorithm iterates between centre assignment (a) and centre update (b) until the maximum number of iterations is reached or cluster assignments do not change.

255   $$C_k = \frac{1}{N_i}\sum_{j=1}^{N_i} x_j, \quad x_k \in A_k,$$ (19)

Where A_k is the subset of D and N_i is the number of samples in A_k.

The K-means model was implemented based on the MATLAB *kmeans* function and the maximum number of iterations was set to 1000 (https://www.mathworks.com/help/stats/kmeans.html). Two sensitive parameters, the number of clusters and the clustering factors, were selected to maximize model performance during the validation procedure.

3.3.2 Heterogeneity measure

The heterogeneity of subgroup delineation is measured by a Davies-Bouldin index (Davies and Bouldin, 1979). This index considers both intra cluster diversity and inter cluster distances. The intra cluster diversity of a cluster *j* is computed as Eq. in (20)

$$S_j = \frac{1}{N_j} \sum_{p_i = j} dis(C_j, x_i)^2, \tag{20}$$

The inter cluster distance between cluster *j* and cluster *k* is measured as Eq. (21):

$$R_{j,k} = \frac{s_j + s_k}{|c_j - c_k|}, \tag{21}$$

The Davies-Bouldin index is computed as Eq. (22) and (23)

$$R_j = \max_{i \neq j}\{R_{j,k}\}, \tag{22}$$

$$DBI = \frac{1}{K} \sum_{j=1}^{K} R_j, \tag{23}$$

Where K is the number of subgroups; DBI is called the Davies–Bouldin index and a lower value means that the subgroups are better clustered.

3.4 Direct regression method

The direct regression method estimates design floods directly with catchment descriptors using a regression model as described in Eq. (24). Three types of regression models were compared in this research and are described below. The optimal regression model for the direct regression method was selected according to the highest prediction accuracy during the validation period. To best of our knowledge, this research is the first time the direct regression method has been tested in an RFFA at the global scale.

$$DF = f_{FQ}(d_1, d_2, \ldots, d_N), \tag{24}$$

Where DF is the design flood for specific return periods; f_{FQ} is the regression model for design flood estimation in each subgroup;

3.4.1 Power-form function (PF)

Power-form (PF) function is a simple non-linear regression model that has been successfully used in RFFA studies at a global scale (Smith et al., 2015). The basic formula of PF regression is described in Eq. (25).

$$DF = \beta_0 x_1^{\beta_1} x_2^{\beta_2} x_3^{\beta_3} \dots x_M^{\beta_M}, \tag{25}$$

285 Where β_m are the model parameters and x_m is the explanatory descriptors used for model development; M is the total number

of the descriptors.

3.4.2 Support vector machine (SVM)

SVM regression has shown advantages in solving complicated non-linear problems in the field of hydrology. For a given

training dataset $\{(x_1, y_1), (x_2, y_2), \dots, (x_N, y_N)\}$, where N is the number of training samples, the overall goal of SVM regression

290 is to find a function $f(x)$ that has at most ε deviation from the observed y_i. Thus, the SVM regression model can be described

as Eq. (26).

$$\min_{w,b,\xi_i,\hat{\xi}_i} \frac{1}{2} \|w\|^2 + C \sum_{i=1}^{N} (\xi_i + \hat{\xi}_i), \tag{26}$$

$$\text{s.t.} \begin{cases} f(x_i) - y_i \leq \varepsilon + \xi_i \\ y_i - f(x_i) \leq \varepsilon + \hat{\xi}_i \\ \xi_i \geq 0, \hat{\xi}_i \geq 0, i = 1,2,\dots,N \end{cases}$$

where ε is the insensitive loss, w and b are hyper-plane parameters; ξ_i and $\hat{\xi}_i$ are two slack variables; and C is a parameter that

295 controls the trade-off between the support line and training samples.

The adopted SVM regression was proposed by Mariette et al. (2015) and the solution of Eq. (26) is described in Garmdareh et

al. (2018);Gizaw and Gan (2016).

3.4.3 Random forest (RF)

RF regression is a representative type of ensemble machine learning model. Unlike SVM, which makes decisions based on a

300 single trained model, RF is based on the average result of numerous independent regression tree models (RTM). In RF, each

RTM is developed with the samples selected by a bootstrap aggregating method from the whole training sample. The out-of-

bag (OOB) samples (samples not selected by the bootstrap method) are applied to test its accuracy. This strategy means RF

usually has good performance in terms of overfitting, outliers and noise. The model structure of RF can be found in the previous

studies (Zhao et al., 2020;Zhao et al., 2018). Once an RTM is developed, the error of OOB samples can be computed (termed

305 E_{OOB1}). Each factor in the OOB samples is permuted one at a time, and the E_{OOB2} can be computed with the permuted OOB

samples and the trained RF model. The RF estimates the factor importance by comparing the difference between E_{OOB1} and

E_{OOB1} while all others are unchanged. The RF has been successfully applied for tasks such as flood assessment, discharge

prediction and ranking of hydrological signatures (Zhao et al., 2018;Hutengs and Vohland, 2016;Li et al., 2016), but this is the

first time the method has been applied in an RFFA to the best of the author's knowledge.

3.5 Validation indices

Two widely used indices, the root mean square normalised error (RMSNE) and the relative mean bias (RBIAS) were applied for model evaluation (Salinas et al., 2013;Shu and Ouarda, 2008;Smith et al., 2015). The RMSNE and RBIAS are computed as in Eq. (27) and (28) respectively. Both RMSNE and RBIAS are negatively oriented indices where lower values mean better model performances. Since the errors in RMSNE are squared before they are averaged, it should be more useful than RBIAS when large errors are particularly undesirable. However, as well as its use in error evaluation, RBIAS can describe if the model has positive bias (underestimation) or negative bias (overestimation).

$$RMSNE = \sqrt{\frac{1}{N}\sum_{i=1}^{N}\left(\frac{q_i-\widehat{q_i}}{q_i}\right)^2}, \tag{27}$$

$$RBIAS = \frac{1}{N}\sum_{i=1}^{N}\left(\frac{q_i-\widehat{q_i}}{q_i}\right), \tag{28}$$

Where q_i is the flood runoff for specific return periods derived by observed data, $\widehat{q_i}$ is the flood runoff for specific return periods estimated by the RFFA method and N is the total number of stations.

4 Results and discussion

4.1 At-site flood estimation

Firstly, 16854 stations with a historical streamflow record of 20 years or longer were selected from all stations in the GSIM archive. Then, the MK, SNHT, and AD tests were applied to these stations. As shown in **Figure 3**, the thresholds of the MK, SNHT and AD tests were derived based on the 95% quantile value of the |Z|, T and A^2 indices, respectively. A total number of 1951 stations which experience obvious trends (or sudden changes), or at which the discharge data did not obey the given hypothetical distributions were not considered further. The selected stations were then clustered into several subgroups based on a K-means clustering model and the discordancy measures described in 3.1.2 were further applied to these stations in each subgroup. Finally, 11793 stations were selected for model development in this research.

Taking one selected station (No. AT0000032) as an example, as shown in **Figure 4** (a), the P3 distribution was selected as the optimal flood frequency curve for this station as this gives the minimal A^2 of 0.43 among all hypothetical distributions. After the flood frequency curve was defined, the parameters and uncertainties of the P3 curve were estimated based on the Bayesian MCMC method described in the section 3.2.2. As shown in **Figure 4** (b), the uncertainties (band between 0.05-0.95 confidence interval) improved with the increase of return periods and the 100-year return period could be estimated within 25% RBIAS for this station. The results of flood frequency curve selection and 100-year return period flood estimation for all stations are shown in **Figure** 4 (c) and (d). We found that P3 and GENLOGIS are two most favoured distributions and only a small percentage of stations obey a NORM distribution. The NORM and GENLOGIS are more suitable for high flow areas and EXP is recommended for low flow areas.
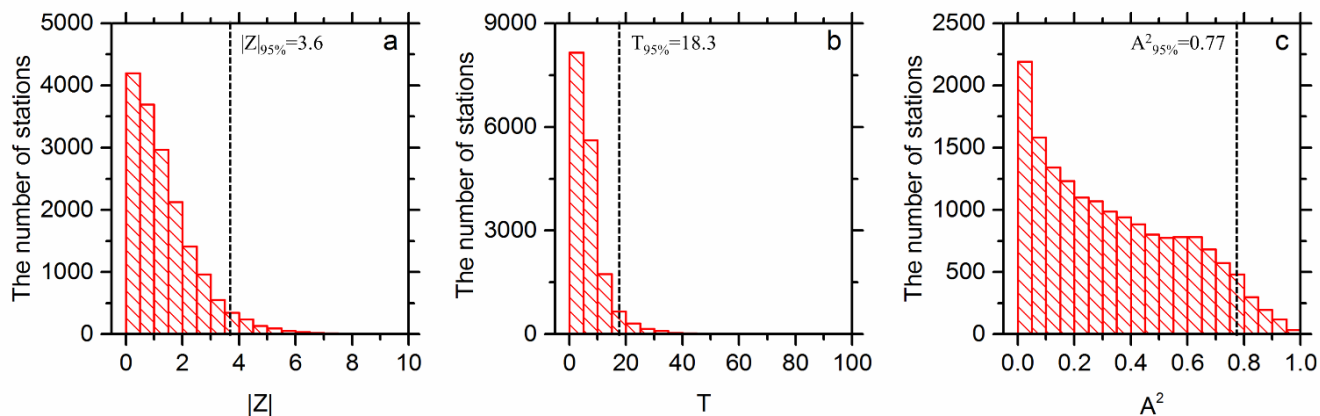
340   **Figure 3 Thresholds for MK (a), SNHT (b) and AD (c) tests during station selection**
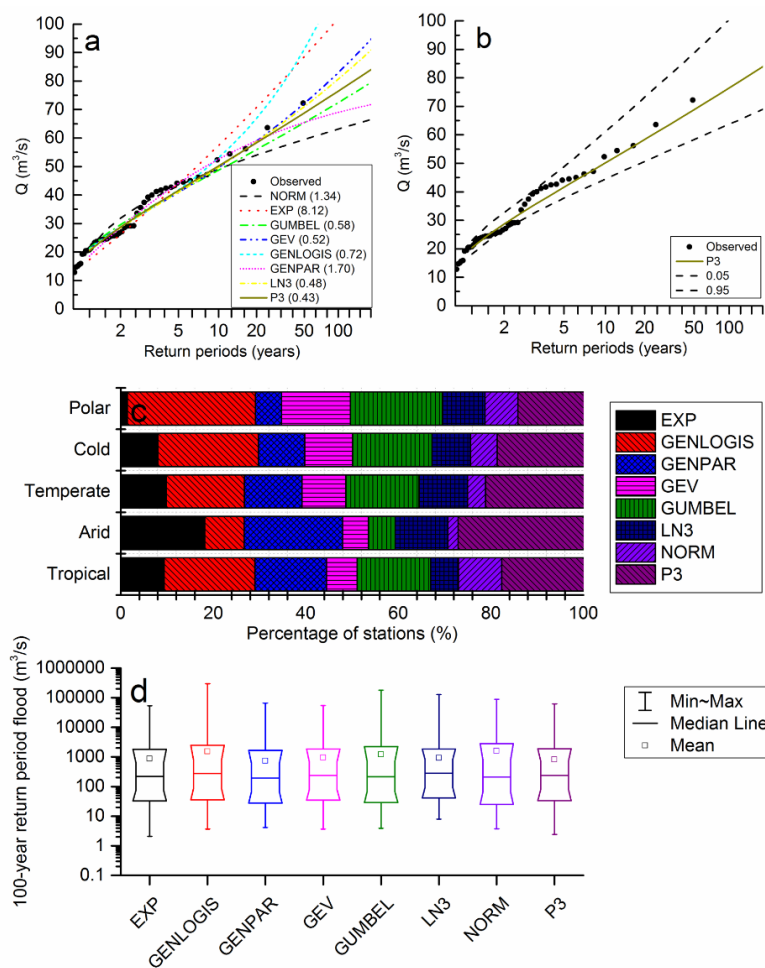
Figure 4 Flood frequency curve selection and estimation

4.2 Subgroups delineation

The selected stations were clustered into several subgroups using the K-means model and an SVM regression model was
345 developed in each subgroup for regional flood estimation. For subgroup delineation, the number of clusters (K) and the
clustering factors are two sensitive parameters. The value of K is selected by considering both the heterogeneity (reflected by
the DB index) and the number of stations in the subgroup. **Figure 5** describes the selection process of K when using all factors
for clustering. As shown in **Figure 5** (a), the DB index reached an optimal value at K=16 and then fluctuated with the increase
of K. From **Figure 5** (b) we found that the number of stations in subgroups reduced with a larger K. To ensure a sufficient
350 number of stations for model development for each subgroup, K greater than 40 is not considered in this research.
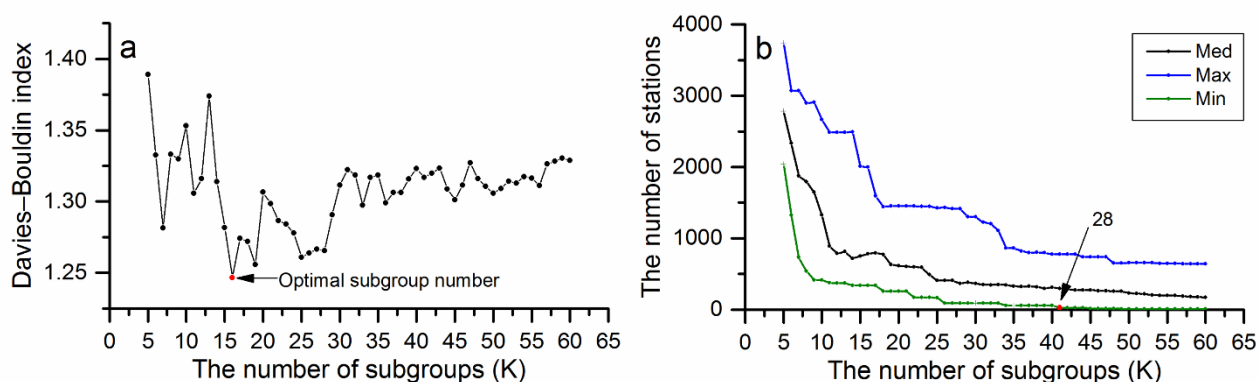
Figure 5 Optimal K selection during subgroups delineation

Taking the 100-year flood estimation as an example, different combinations of clustering factors were tested using the optimal
K. As shown in **Table 4**, the best combination is to use all factors for clustering, and this result reaches the best RRMSE of
355 0.708 and RBIAS of -0.174 among all combinations for the validation periods. The design flood still could be satisfactorily
estimated (RBIAS<0.25) when using meteorological, physiographical, or hydrological factors for clustering, respectively.
Anthropological factors alone are not recommended for clustering as this results in the worst RMSNE of 1.788 and RBIAS of
-0.909 among all combinations.

Table 4 The impact of clustering factors on regional 100-year flood estimation

Clustering factors	Optimal K	Training		Validation	
		RBIAS	RMSNE	RBIAS	RMSNE
All factors	16	-0.179	0.703	-0.174	0.708
Meteorological factors	11	-0.202	0.768	-0.185	0.746
Physiographical factors	5	-0.214	0.829	-0.244	0.824
Hydrological factors	30	-0.207	0.781	-0.243	0.876
Anthropological factors	7	-0.379	1.235	-0.909	1.788

4.3 Regression model comparison

Three regression models, PF, SVM, and RF were compared for 100-year flood estimation. **Figure 6** describes the accuracy of the three models during training and validation periods. We found that PF showed the worse accuracy with RMSNE of 1.175 and 1.1089 in training and validation periods respectively. RF gave the highest fitting ability during the training period with the RMSNE of 0.290 and RBIAS of -0.037. However, the SVM model outperformed the RF model during the validation period with the RMSNE of 0.708 and RBIAS of -0.174. Therefore, SVM was selected for flood estimation for ungauged areas in this research.
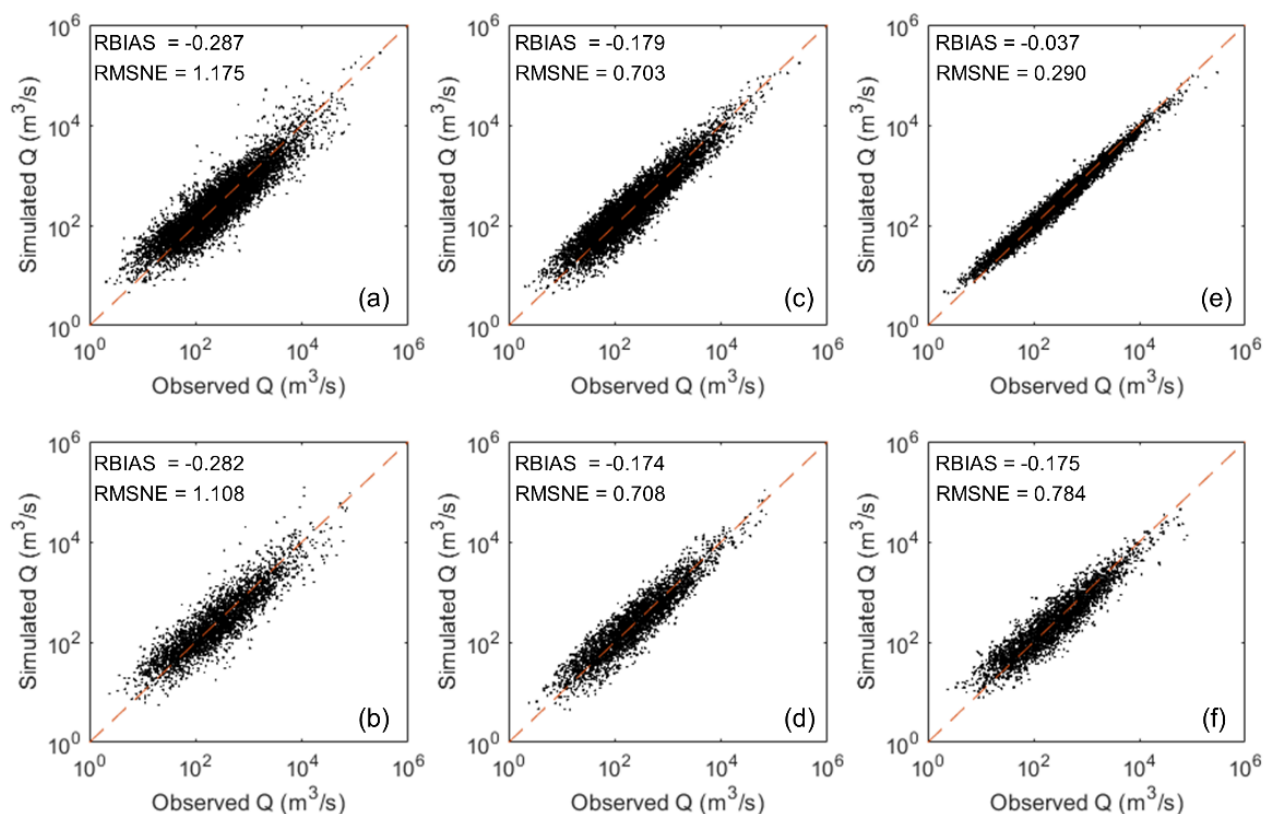
Figure 6 Comparison of three regression models during training and validation periods
(a): PF training; (b): PF testing; (a): SVM training; (b): SVM testing; (a): RF training; (b): RF testing

The factor importance in each subgroup was evaluated using the RF model and **Figure 7** (a) describes the average value of factor importance of all subgroups. The top five important factors are the catchment area (CA) and annual precipitation (AP), Longitude (LO) and latitude (LA) and temperature range (TR). Meanwhile, population density (PD) and dam capacity (DC) and curve number (CN) are the three least important factors and make up a relatively low proportion (< 5%) of the total importance among all factors.
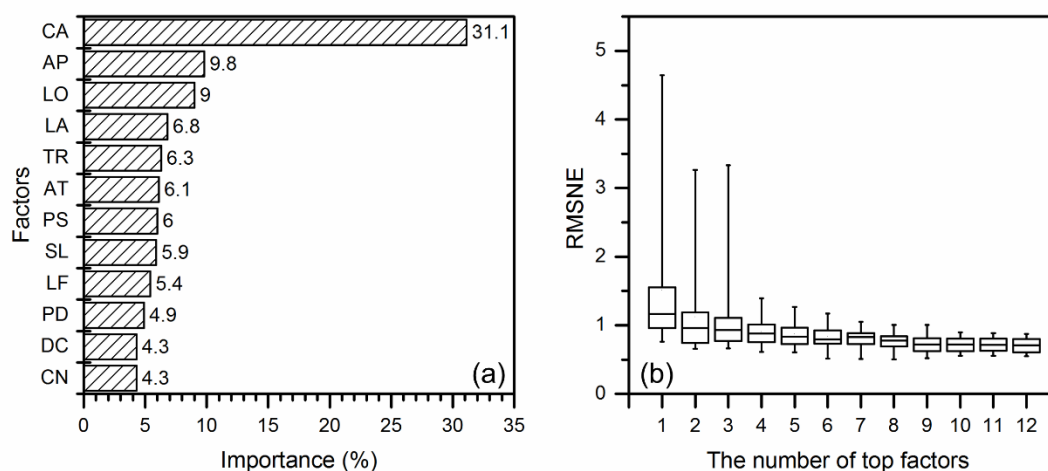
Figure 7 (a) Factor importance evaluated by RF model and (b) the impact of catchment descriptors for regression

The impact of catchment descriptors on regression results was tested based on the optimal SVM regression and the factor importance order identified by the RF model. **Figure 7** (b) described the RMSNE for all subgroups during the validation period considering different combinations of catchment descriptors. AP and CA are the two most important factors and also were recommended as the catchment descriptors in the global RFFA approach of Smith et al. (2015) with a small number of samples (242 stations) for validation. When only using the CA and AP (top 2 factors) for regression and a large number of stations (3485 stations) for validation, the design flood cannot be accurately estimated for some subgroups (RMSNE>1.0). As shown in **Figure 7 (b),** the prediction accuracy can be improved by considering more importance factors for model training and validation. After considering the top 10 factors for regression, the RMSNE of subgroups becomes stable and does not significantly improved by adding the further factors DC and CN. The SVM showed the highest performance considering all factors for regression (mean RMSNE of 0.708 in the validation period).

4.4 Regional flood estimation

Figure 8 (a-e) demonstrates the simulated results from the optimal SVM model in each climate zone and **Figure 8** (f) displays the cumulative distribution function (CDF) between the simulated and observed discharge for all stations. Specially, the RMSNEs found were 0.746, 0.785, 0.722, 0.704 and 0.480 for tropical, arid, temperate, cold, polar climates respectively. Although there were some large individual error points, the SVM model showed good performance in tropical, temperature, cold and polar climate zones with an RBIAS of -0.199, -0.169, -0.179 and -0.091 respectively. The SVM model showed a higher error of flood estimation in arid zones with an RBIAS of -0.233. As shown in **Figure 8** (f), the simulated result can successfully fit the observed discharge curve given its likely error. However, some overestimation was found at low discharges, which is also reflected in the negative value of RBIAS during evaluation. It is logical that modelled values are usually less dispersed than observed values as the training target focuses on the mean value. Moreover, the catchment descriptors derived

375

380

385

390

395

from global satellite images can have large uncertainties (McCabe et al., 2017) when describing small catchments and can lead to more substantial errors at low discharge.
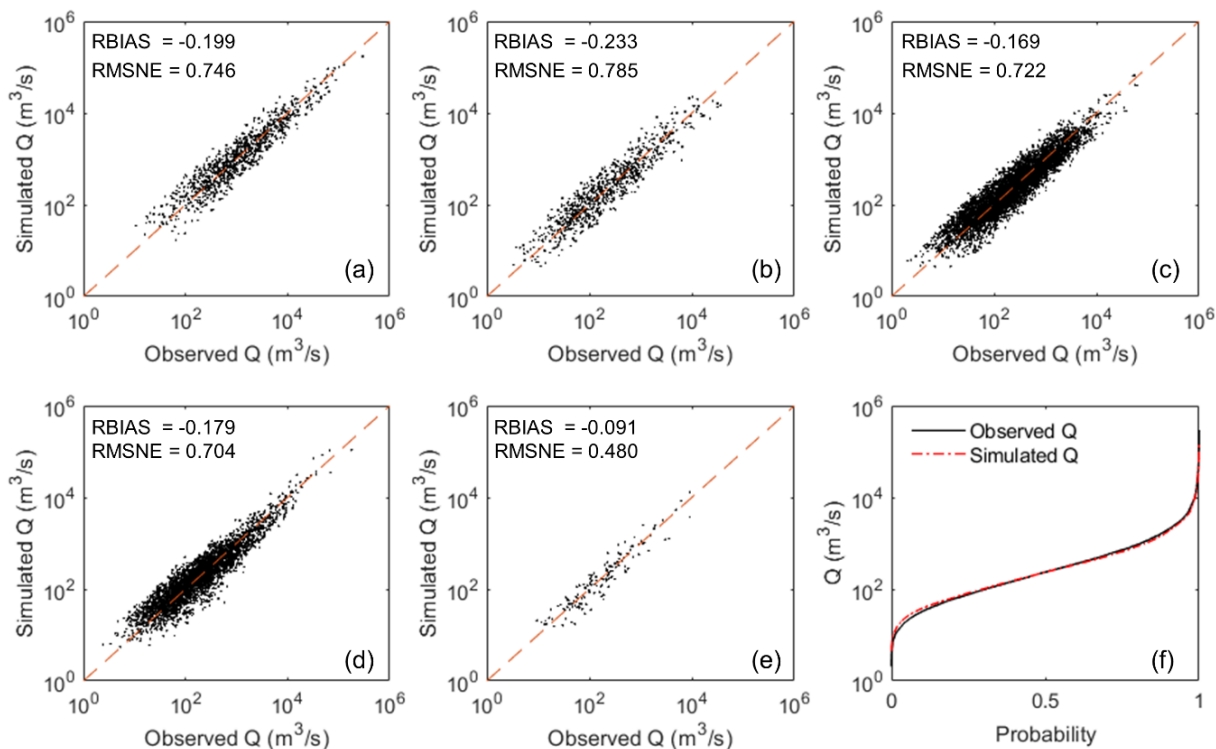
400 **Figure 8 Results of simulated Q100 in different climate zones (a) Tropical; (b) Arid; (c) Temperate; (d) Cold; (e) Polar; (f) Cumulative distribution function of simulated and observed discharge.**

Table 5 Result for different return period flood estimation

Return periods	Training		Testing	
	Mean BIAS	Mean RMSE	Mean BIAS	Mean RMSE
10	-0.160	0.655	-0.165	0.664
20	-0.165	0.663	-0.168	0.672
50	-0.175	0.695	-0.166	0.684
100	-0.179	0.703	-0.174	0.708

Table 5 compares the training and validation results of 10, 20, 50, and 100-year return period floods derived by the proposed direct regression method. By using the proposed direct regression method, all design floods could be estimated within the

405 RBIAS of 0.18 (18%). We found, unsurprisingly, that the prediction accuracy decreases with a larger flood magnitude. This mainly because the at-site design flood derived by observed data is still not truth and large return period floods are more difficult to be reliably estimated with limited observed data (Gaume, 2018). Regarding the natural and epistemic uncertainties

in flood frequency analysis, the RBIAS of at-site design flood estimation was reported as large as 0.30 in some studies (Di Baldassarre et al., 2012;Di Baldassarre and Montanari, 2009;Halbert et al., 2016;Merz and Thieken, 2005). As the at-site

410   design flood is regarded as a training target, this error will be introduced in the regression and will directly affect the approach accuracy. Therefore, RBIAS of 20% or less is very impressive considering the uncertainties of at-site design flood estimation.

Compared with the global RFFA of Smith (2015), this study significantly improved the station density and model accuracy in all climate zones. The proposed approach achieved similar performances to some regional studies by adopting a global coverage of stations (Shu and Ouarda, 2008;Salinas et al., 2013). However, there can still be large errors in design flood

415   estimation, especially in arid zone. This is consistent with previous research and is likely to be a result of dryer regions being more heterogeneous (Salinas et al., 2013;Smith et al., 2015). In this study, the subgroups are delineated based on a K-means model considering at-site explanatory factors. Therefore, the subgroups are not necessarily spatially consistent with climate zone and it may be difficult to properly reflect the heterogeneous characteristics of climate zones. This limitation is also noted in Dallaire et al. (2019) and could be improved by combining the unsupervised and supervised clustering models for subgroup

420   delineation.

5 Conclusions

A three-phase machine learning model-based approach was proposed to estimate design floods along river networks at the global scale. The at-site floods for global gauging station data were estimated based on Bayesian MCMC method. The global stations were then clustered into several subgroups using a K-means clustering model and SVM regression were developed in

425   each subarea for design flood estimation. Three widely used regression techniques, Power-form function (PF), Support Vector Machine (SVM) and Random Forests (RF), were compared for regression in each subgroup. The regional floods were final estimated with the using the same descriptors and the optimal SVM regression model.

The main conclusions of this study are summarised below:

(1)   To make reliable estimates, 11793 stations from the GSIM archive were selected for model implementation using

430   stationarity, discordancy and homogeneity measures. For clustering, the impact of clustering number and clustering factors on estimation accuracy were tested. The best clustering number (K) was 16 which gave the lowest RMSNE of 0.708 for 100-year flood estimation when using all factors for clustering in a K-means model.

(2)   Three regression models were compared for 100-year flood estimation and the SVM method showed the highest accuracy during the validation period with the RMSNE of 0.708 and RBIAS of -0.174. Factor importance was identified using the

435   RF model, and different combinations of factors were tested for the optimal SVM regression implementation. When only using the top 2 factors (annual precipitation and catchment area) for regression and a large number of stations (3485 stations) for validation, the design flood cannot be accurately estimated (RMSNE>1.0) for some subgroups. After considering the top 10 factors for regression, the RMSNE for subgroups become stable and did not significantly improve by further adding factors.

440 (3) The proposed approach showed good performance in tropical, temperate, cold, and polar climate zones with an RBIAS of -0.199, -0.169, -0.179 and -0.091 respectively (i.e. the bias was less than 20%). A satisfying performance was found in arid areas with an RBIAS of -0.233. The negative value of RBIAS reflected some overestimation which mainly occurred due to low discharge in small catchments.

This approach shows considerable promise for the estimation of extreme flood magnitudes at global scales and average RBIAS
445 in estimation is less than 18% for all design floods. This is likely to yield a significant improvement in the skill of global flood inundation models.

6 Code availability

The MKT and SNHT were implemented using the *trend* package (https://CRAN.R-project.org/package=trend). The discorda ncy and at-site design floods were estimated based on the nsRFA package (https://CRAN.R-project.org/package=nsRFA). Th
450 e heterogeneity measure, K-means, SVM and RF models are available from https://www.mathworks.com/help/stats/kmeans. html, https://uk.mathworks.com/help/stats/support-vector-machine-regression.html, and https://www.stat.berkeley.edu/~brei man/RandomForests/ respectively.

7 Data availability

The Global Streamflow Indices and Metadata Archive (GSIM) is freely available at https://doi.pangaea.de/10.1594/PANGA
455 EA.887477. To access WorldClim - Global Climate Data, visit http://www.worldclim.org/. The adopted terrain data is the M ERIT-DEM at http://hydro.iis.u-tokyo.ac.jp/~yamadai/MERIT_DEM/. The Gridded Population of the World (GPW) dataset is available from https://sedac.ciesin.columbia.edu/data/collection/gpw-v4. The Global Lakes and Wetlands Database (GLW D) is available from https://www.worldwildlife.org/pages/global-lakes-and-wetlands-database. The data sources of NRCS Cu rve Number dataset is described at https://doi.org/10.1080/2150704X.2017.1297544. The Global Reservoir and Dam Databas
460 e (GRanD) can be downloaded by visiting http://globaldamwatch.org/grand/.

8 Author contribution

Conceptualization: Gang Zhao, Paul Bates and Jeff Neal; Methodology: Gang Zhao; Formal analysis: Gang Zhao; Writing-original draft preparation: Gang Zhao; writing—review and editing: Paul Bates, Jeff Neal and Bo Pang; Visualization, Gang Zhao; Supervision, Paul Bates and Jeff Neal;

465 ## 9 Competing interests

The authors declare that they have no conflict of interest.

10 Acknowledgments

Gang Zhao would like to thank Andrew Smith at Fathom for helpful discussions. Paul Bates is supported by a Royal Society

Wolfson Research Merit award. Jeff Neal is supported by NERC grants (NE/S003061/1 and NE/S006079/1). Gang Zhao is s

470 upported by the China Scholarship Council-University of Bristol Joint PhD Scholarships Programme (No.201700260088). B

o Pang is supported by National Natural Science Foundation of China (No. 51879008).

Referecnes

Ahmad, M. I., Sinclair, C., and Spurr, B.: Assessment of flood frequency models using empirical distribution function statistics, Water Resour Res, 24, 1323-1328, 1988.

475 Alexandersson, H.: A Homogeneity Test Applied to Precipitation Data, J Climatol, 6, 661-675, DOI 10.1002/joc.3370060607, 1986.

Bocchiola, D., De Michele, C., Rosso, R. J. H., and Discussions, E. S. S.: Review of recent advances in index flood estimation, 7, 283-296, 2003.

CRED, and UNISDR: The Human Cost of Weather Related Disasters - 1995 - 2015, United Nations Office for Disaster Risk

480 Reduction (UNISDR) and Centre for Research on the Epidemiology of Disasters (CRED), 2015.

Cunnane, C.: Methods and Merits of Regional Flood Frequency-Analysis, J Hydrol, 100, 269-290, Doi 10.1016/0022-1694(88)90188-6, 1988.

Dallaire, C. O., Lehner, B., Sayre, R., and Thieme, M.: A multidisciplinary framework to derive global river reach classifications at high spatial resolution, Environ Res Lett, 14, 024003, 2019.

485 Dalrymple, T.: Flood-frequency analyses, manual of hydrology: Part 3, USGPO, 1960.

Davies, D. L., and Bouldin, D. W.: A cluster separation measure, IEEE transactions on pattern analysis and machine intelligence, 224-227, 1979.

Di Baldassarre, G., and Montanari, A.: Uncertainty in river discharge observations: a quantitative analysis, Hydrology & Earth System Sciences, 13, 2009.

490 Di Baldassarre, G., Laio, F., and Montanari, A.: Effect of observation errors on the uncertainty of design floods, Physics and Chemistry of the Earth, Parts A/B/C, 42, 85-90, 2012.

Do, H., Zhao, F., Westra, S., Leonard, M., and Gudmundsson, L.: A global-scale comparison of modeled and observed trends in magnitude and frequency of flooding, Geophysical Research Abstracts, 2019,

Do, H. X., Gudmundsson, L., Leonard, M., and Westra, S.: The Global Streamflow Indices and Metadata Archive (GSIM) -

495 Part 1: The production of a daily streamflow archive and metadata, Earth Syst Sci Data, 10, 10.5194/essd-10-765-2018, 2018.

Doxsey-Whitfield, E., MacManus, K., Adamo, S. B., Pistolesi, L., Squires, J., Borkovska, O., and Baptista, S. R. J. P. i. A. G.: Taking advantage of the improved availability of census data: a first look at the gridded population of the world, version 4, 1, 226-234, 2015.

500 Fick, S. E., and Hijmans, R. J.: WorldClim 2: new 1-km spatial resolution climate surfaces for global land areas, Int J Climatol, 37, 4302-4315, 10.1002/joc.5086, 2017.

Frieler, K., Lange, S., Piontek, F., Reyer, C. P., Schewe, J., Warszawski, L., Zhao, F., Chini, L., Denvil, S., and Emanuel, K. J. G. M. D.: Assessing the impacts of 1.5 C global warming–simulation protocol of the Inter-Sectoral Impact Model Intercomparison Project (ISIMIP2b), 2017.

505 Garcia, F. A. A.: Tests to identify outliers in data series, Pontifical Catholic University of Rio de Janeiro, Industrial Engineering Department, Rio de Janeiro, Brazil, 2012.

Garmdareh, E. S., Vafakhah, M., and Eslamian, S. S.: Regional flood frequency analysis using support vector regression in arid and semi-arid regions of Iran, Hydrolog Sci J, 63, 426-440, 10.1080/02626667.2018.1432056, 2018.

Gaume, E.: Flood frequency analysis: The Bayesian choice, Wiley Interdisciplinary Reviews: Water, 5, e1290, 2018.

510 Gizaw, M. S., and Gan, T. Y.: Regional flood frequency analysis using support vector regression under historical and future climate, J Hydrol, 538, 387-398, 2016.

Griffis, V. W., and Stedinger, J. R.: Log-Pearson Type 3 distribution and its application in flood frequency analysis. I: Distribution characteristics, J Hydrol Eng, 12, 482-491, 10.1061/(Asce)1084-0699(2007)12:5(482), 2007.

Gudmundsson, L., Do, H. X., Leonard, M., and Westra, S.: The Global Streamflow Indices and Metadata Archive (GSIM) - Part 2: Quality control, time-series indices and homogeneity assessment, Earth Syst Sci Data, 10, 10.5194/essd-10-787-2018, 2018.

Haddad, K., and Rahman, A.: Selection of the best fit flood frequency distribution and parameter estimation procedure: a case study for Tasmania in Australia, Stochastic Environmental Research and Risk Assessment, 25, 415-428, 2011.

Halbert, K., Nguyen, C. C., Payrastre, O., and Gaume, E.: Reducing uncertainty in flood frequency analyses: A comparison of local and regional approaches involving information on extreme historical floods, J Hydrol, 541, 90-98, 2016.

Hamed, K. H. J. J. o. h.: Trend detection in hydrologic data: the Mann–Kendall trend test under the scaling hypothesis, 349, 350-363, 2008.

Hammond, M. J., Chen, A. S., Djordjevic, S., Butler, D., and Mark, O.: Urban flood impact assessment: A state-of-the-art review, Urban Water J, 12, 14-29, 10.1080/1573062x.2013.857421, 2015.

Hosking, J. R. M., and Wallis, J. R.: The Effect of Intersite Dependence on Regional Flood Frequency-Analysis, Water Resour Res, 24, 588-600, DOI 10.1029/WR024i004p00588, 1988.

Hosking, J. R. M., and Wallis, J. R.: Regional frequency analysis: an approach based on L-moments, Cambridge University Press, 2005.

Hutengs, C., and Vohland, M.: Downscaling land surface temperatures at regional scales with random forest regression, Remote Sens Environ, 178, 127-141, 10.1016/j.rse.2016.03.006, 2016.

Kundzewicz, Z. W., Kanae, S., Seneviratne, S. I., Handmer, J., Nicholls, N., Peduzzi, P., Mechler, R., Bouwer, L. M., Arnell, N., Mach, K., Muir-Wood, R., Brakenridge, G. R., Kron, W., Benito, G., Honda, Y., Takahashi, K., and Sherstyukov, B.: Flood risk and climate change: global and regional perspectives, Hydrolog Sci J, 59, 1-28, 10.1080/02626667.2013.857411, 2014.

Laio, F.: Cramer–von Mises and Anderson-Darling goodness of fit tests for extreme value distributions with unknown parameters, Water Resour Res, 40, 2004.

Lehner, B., and Doll, P.: Development and validation of a global database of lakes, reservoirs and wetlands, J Hydrol, 296, 1-22, 10.1016/j.jhydrol.2004.03.028, 2004.

Lehner, B., Liermann, C. R., Revenga, C., Vorosmarty, C., Fekete, B., Crouzet, P., Doll, P., Endejan, M., Frenken, K., Magome, J., Nilsson, C., Robertson, J. C., Rodel, R., Sindorf, N., and Wisser, D.: High-resolution mapping of the world's reservoirs and dams for sustainable river-flow management, Front Ecol Environ, 9, 494-502, 10.1890/100125, 2011.

Li, B., Yang, G. S., Wan, R. R., Dai, X., and Zhang, Y. H.: Comparison of random forests and other statistical methods for the prediction of lake water level: a case study of the Poyang Lake in China, Hydrol Res, 47, 69-83, 10.2166/nh.2016.264, 2016.

Lin, G. F., and Chen, L. H.: Identification of homogeneous regions for regional frequency analysis using the self-organizing map, J Hydrol, 324, 1-9, 10.1016/j.jhydrol.2005.09.009, 2006.

Liu, X., Liu, W., Yang, H., Tang, Q., Flörke, M., Masaki, Y., Müller Schmied, H., Ostberg, S., Pokhrel, Y., and Satoh, Y.: Multimodel assessments of human and climate impacts on mean annual streamflow in China, Hydrol Earth Syst Sc, 23, 1245-1261, 2019.

McCabe, M. F., Rodell, M., Alsdorf, D. E., Miralles, D. G., Uijlenhoet, R., Wagner, W., Lucieer, A., Houborg, R., Verhoest, N. E., and Franz, T. E.: The future of Earth observation in hydrology, Hydrol Earth Syst Sc, 21, 3879, 2017.

Merz, B., and Thieken, A. H.: Separating natural and epistemic uncertainty in flood frequency analysis, J Hydrol, 309, 114-132, 2005.

Merz, R., and Bloschl, G.: Flood frequency hydrology: 2. Combining data evidence, Water Resour Res, 44, Artn W0843310.1029/2007wr006745, 2008a.

Merz, R., and Bloschl, G.: Flood frequency hydrology: 1. Temporal, spatial, and causal expansion of information, Water Resour Res, 44, Artn W0843210.1029/2007wr006744, 2008b.

Mockus, V.: National engineering handbook, Section, 1964.

560   Mueller Schmied, H., Adam, L., Eisner, S., Fink, G., Flörke, M., Kim, H., Oki, T., Portmann, F. T., Reinecke, R., Riedel, C.
      J. H., and Sciences, E. S.: Variations of global and continental water balance components as impacted by climate
      forcing uncertainty and human water use, 20, 2877-2898, 2016.
      Nazmi, N., Saipol, H., Yusof, F., Mazlan, S., Rahman, M., Nordin, N., Johari, N., and Aziz, S.: Parameter Estimation of
      Extreme Rainfall Distribution in Johor using Bayesian Markov Chain Monte Carlo, IOP Conference Series: Earth and
565   Environmental Science, 2020, 012019,
      Prihodko, L., Denning, A. S., Hanan, N. P., Baker, I., and Davis, K.: Sensitivity, uncertainty and time dependence of
      parameters in a complex land surface model, Agr Forest Meteorol, 148, 268-287, 10.1016/j.agrformet.2007.08.006,
      2008.
      Reis, D. S., and Stedinger, J. R.: Bayesian MCMC flood frequency analysis with historical information, J Hydrol, 313, 97-
570   116, 2005.
      Richter, B. D., Baumgartner, J. V., Wigington, R., and Braun, D. P.: How much water does a river need?, Freshwater Biol,
      37, 231-249, DOI 10.1046/j.1365-2427.1997.00153.x, 1997.
      Salinas, J. L., Laaha, G., Rogger, M., Parajka, J., Viglione, A., Sivapalan, M., and Blöschl, G.: Comparative assessment of
      predictions in ungauged basins – Part 2: Flood and low flow studies, Hydrol. Earth Syst. Sci., 17, 2637-2652,
575   10.5194/hess-17-2637-2013, 2013.
      Sampson, C. C., Smith, A. M., Bates, P. B., Neal, J. C., Alfieri, L., and Freer, J. E.: A high-resolution global flood hazard
      model, Water Resour Res, 51, 7358-7381, 10.1002/2015wr016954, 2015.
      Schumann, G. J.-P., Andreadis, K. M., and Bates, P. D. J. J. o. h.: Downscaling coarse grid hydrodynamic model simulations
      over large domains, 508, 289-298, 2014a.
580   Schumann, G. J. P., Neal, J. C., Voisin, N., Andreadis, K. M., Pappenberger, F., Phanthuwongpakdee, N., Hall, A. C., and
      Bates, P. D.: A first large-scale flood inundation forecasting model, Water Resour Res, 49, 6248-6257,
      10.1002/wrcr.20521, 2013.
      Schumann, G. J. P., Andreadis, K. M., and Bates, P. D.: Downscaling coarse grid hydrodynamic model simulations over
      large domains, J Hydrol, 508, 289-298, 10.1016/j.jhydrol.2013.08.051, 2014b.
585   Shiffler, R. E. J. T. A. S.: Maximum Z scores and outliers, 42, 79-80, 1988.
      Shu, C., and Ouarda, T. B. M. J.: Regional flood frequency analysis at ungauged sites using the adaptive neuro-fuzzy
      inference system, J Hydrol, 349, 31-43, 10.1016/j.jhydrol.2007.10.050, 2008.
      Smith, A., Sampson, C., and Bates, P.: Regional flood frequency analysis at the global scale, Water Resour Res, 51, 539-
      553, 10.1002/2014wr015814, 2015.
590   Stedinger, J. R.: Estimating a regional flood frequency distribution, Water Resour Res, 19, 503-510, 1983.
      Stein, L., Pianosi, F., and Woods, R.: Event-based classification for global study of river flood generating processes, Hydrol
      Process, 2019.
      Teng, J., Jakeman, A. J., Vaze, J., Croke, B. F. W., Dutta, D., and Kim, S.: Flood inundation modelling: A review of
      methods, recent advances and uncertainty analysis, Environ Modell Softw, 90, 201-216, 10.1016/j.envsoft.2017.01.006,
595   2017.
      Trigg, M. A., Birch, C. E., Neal, J. C., Bates, P. D., Smith, A., Sampson, C. C., Yamazaki, D., Hirabayashi, Y.,
      Pappenberger, F., Dutra, E., Ward, P. J., Winsemius, H. C., Salamon, P., Dottori, F., Rudari, R., Kappes, M. S.,
      Simpson, A. L., Hadzilacos, G., and Fewtrell, T. J.: The credibility challenge for global fluvial flood risk analysis,
      Environ Res Lett, 11, Artn 09401410.1088/1748-9326/11/9/094014, 2016.
600   Vogel, R. M., McMahon, T. A., and Chiew, F. H.: Floodflow frequency model selection in Australia, J Hydrol, 146, 421-
      449, 1993a.
      Vogel, R. M., Thomas Jr, W. O., and McMahon, T. A.: Flood-flow frequency model selection in southwestern United States,
      Journal of Water Resources Planning and Management, 119, 353-366, 1993b.
      Wing, O. E., Bates, P. D., Sampson, C. C., Smith, A. M., Johnson, K. A., and Erickson, T. A. J. W. R. R.: Validation of a 30
605   m resolution flood hazard model of the conterminous U nited S tates, 53, 7968-7986, 2017.
      Wing, O. E., Bates, P. D., Smith, A. M., Sampson, C. C., Johnson, K. A., Fargione, J., and Morefield, P.: Estimates of
      present and future flood risk in the conterminous United States, Environ Res Lett, 13, 034023, 2018a.

Wing, O. E. J., Bates, P. D., Smith, A. M., Sampson, C. C., Johnson, K. A., Fargione, J., and Morefield, P.: Estimates of present and future flood risk in the conterminous United States, Environ Res Lett, 13, ARTN 03402310.1088/1748-9326/aaac65, 2018b.

Winsemius, H., Van Beek, L., Jongman, B., Ward, P., and Bouwman, A.: A framework for global river flood risk assessments, 2013.

Winsemius, H. C., Aerts, J. C., Van Beek, L. P., Bierkens, M. F., Bouwman, A., Jongman, B., Kwadijk, J. C., Ligtvoet, W., Lucas, P. L., and Van Vuuren, D. P.: Global drivers of future river flood risk, Nat Clim Change, 6, 381-385, 2016a.

Winsemius, H. C., Aerts, J. C. J. H., van Beek, L. P. H., Bierkens, M. F. P., Bouwman, A., Jongman, B., Kwadijk, J. C. J., Ligtvoet, W., Lucas, P. L., van Vuuren, D. P., and Ward, P. J.: Global drivers of future river flood risk, Nat Clim Change, 6, 381-385, 10.1038/Nclimate2893, 2016b.

Yamazaki, D., Kanae, S., Kim, H., and Oki, T.: A physically based description of floodplain inundation dynamics in a global river routing model, Water Resour Res, 47, Artn W0450110.1029/2010wr009726, 2011.

Yamazaki, D., Ikeshima, D., Tawatari, R., Yamaguchi, T., O'Loughlin, F., Neal, J. C., Sampson, C. C., Kanae, S., and Bates, P. D.: A high-accuracy map of global terrain elevations, Geophys Res Lett, 44, 5844-5853, 10.1002/2017gl072874, 2017.

Yang, T., Sun, F., Gentine, P., Liu, W., Wang, H., Yin, J., Du, M., and Changming, L.: Evaluation and machine learning improvement of global flood simulations, AGUFM, 2019, H33L-2122, 2019a.

Yang, T., Sun, F., Gentine, P., Liu, W., Wang, H., Yin, J., Du, M., and Liu, C.: Evaluation and machine learning improvement of global hydrological model-based flood simulations, Environ Res Lett, 14, 114027, 2019b.

Zeng, Z. Y., Tang, G. Q., Hong, Y., Zeng, C., and Yang, Y.: Development of an NRCS curve number global dataset using the latest geospatial remote sensing data for worldwide hydrologic applications, Remote Sens Lett, 8, 528-536, 10.1080/2150704x.2017.1297544, 2017.

Zhang, Y., Chiew, F. H., Li, M., and Post, D.: Predicting runoff signatures using regression and hydrological modeling approaches, Water Resour Res, 54, 7859-7878, 2018.

Zhao, G., Pang, B., Xu, Z. X., Yue, J. J., and Tu, T. B.: Mapping flood susceptibility in mountainous areas on a national scale in China, Sci Total Environ, 615, 1133-1142, 10.1016/j.scitotenv.2017.10.037, 2018.

Zhao, G., Bates, P., and Neal, J.: The impact of dams on design floods in the Conterminous US, Water Resour Res, 56, e2019WR025380, 2020.